Modulation of Magainin 2−Lipid Bilayer Interactions by Peptide Charge†

Katsumi Matsuzaki,* Akemi Nakamura, Osamu Murase, Ken-ichi Sugishita, Nobutaka Fujii, and Koichiro Miyajima

Faculty of Pharmaceutical Sciences, Kyoto University, Sakyo-ku, Kyoto 606-01, Japan

Received July 29, 1996; Revised Manuscript Received November 4, 1996⊗

ABSTRACT: Magainin 2, an antimicrobial peptide from *Xenopus* skin, assumes an amphiphilic helix when bound to acidic phospholipids, forming a pore composed of a dynamic, peptide−lipid supramolecular complex [Matsuzaki et al. (1996) *Biochemistry 35*, 11361−11368]. Upon the disintegration of the pore, a fraction of the peptide molecules stochastically translocates across the bilayer (Matsuzaki, et al., 1995). In order to investigate the effects of peptide charge on the magainin 2−lipid bilayer interactions, we synthesized four magainin 2 analogs with different charges (0−6+). MG0: K10E, K11E, F12W-magainin 2. MG2+: K10E, F12W-magainin 2. MG4+: F12W-magainin 2. MG6+: F12W, E19Q-magainin 2 amide. An increase in charge resulted in a stronger binding of the peptide to the negatively charged membranes, suggesting that electrostatic attractions play a crucial role in the binding process. The helical stability in a trifluoroethanol/buffer mixture was decreased with increasing positive charge because of electrostatic repulsions between the closely spaced positive side chains, whereas the helicity in the lipid bilayer was much higher and appeared to be independent of the peptide charge. However, enhanced repulsions between the highly positively charged helices destabilized the pore. Therefore, the efficiency of the most basic peptide (MG6+) to translocate across the bilayer was the greatest by virtue of the short life span of its pore and the very tight membrane binding. The charge distribution of wild-type magainin 2 was found to be so designed as to exhibit the maximal lytic activity by simultaneously achieving a strong binding and a moderate pore stability.

Magainin 2 (GIGKFLHSAKKFGKAFVGEIMNS), isolated from the skin of *Xenopus laevis*, is a self-defense peptide with a broad spectrum of antimicrobial activity (Zasloff, 1987), and a promising candidate of a new antibiotic of therapeutic value (Maloy & Kari, 1995). The peptide is considered to kill its target cells by permeabilizing their membranes. The lipid matrix appears to be the site of action: the all-D-enantiomer is fully active compared with the parent all-L-peptide, suggesting that chiral proteins are not involved in the exhibition of the activity (Wade et al., 1990). Magainin 2 induces the efflux of water soluble molecules entrapped within artificial lipid vesicles (Matsuzaki et al., 1991; Grant et al., 1992; Vaz Gomes et al., 1993). The dependence of the peptide's lytic activity on the lipid species can well explain the selectivity of its action for various types of cells (Matsuzaki et al., 1995c). Therefore, a number of studies on magainin−lipid interactions have been performed to elucidate the molecular details of its action mechanism. We propose the following model (Figure 1): (1) Magainin 2 takes unordered structures in an aqueous solution, whereas it forms an amphiphilic helix upon membrane binding. Electrostatic interactions between the peptide's positive charge and the negative charge of the membrane surface play a crucial role in the binding process (Matsuzaki et al., 1991; Vaz Gomes et al., 1993). The affinity for zwitterionic phospholipids is weak because of the peptide's low hydrophobicity, which is responsible for its weak hemolytic activity (Matsuzaki et al., 1995c).

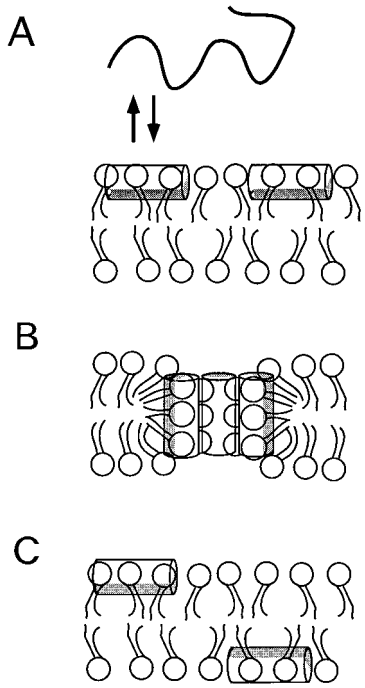

FIGURE 1: A model for magainin 2−lipid bilayer interactions (Matsuzaki, 1995a,b, 1996). (A) Membrane binding accompanying helix formation. The shaded area represents the hydrophobic surface of the amphiphilic helix. (B) Formation of the pore composed of a dynamic, peptide−lipid supramolecular complex. (C) Translocation of the peptide into the inner leaflet upon the disintegration of the pore. See the text for details.

† Supported by The Naito Foundation and Grant-in-Aids for Scientific Research on Priority Areas (No. 08219223) and for Encouragement of Young Scientists (No. 08772061) from the Ministry of Education, Science and Culture of Japan.

* Author to whom correspondence should be addressed. Telephone: 81 75 753 4574. Fax: 81 75 761 2698. E-mail: katsumim@pharm.kyoto-u.ac.jp.

⊗ Abstract published in *Advance ACS Abstracts,* February 1, 1997.

S0006-2960(96)01870-3 CCC: $14.00

Table 1: Amino Acid Sequences and Helical Properties of Magainin 2 Analogs

designation	sequence[a]	charge[b]	$[\theta]_{222}$[c] membrane[d]	$[\theta]_{222}$[c] TFE/buffer[e]	ΔH (J/mol)[f]	T_m (K)[g]
MG0	GIGKFLHSAEEWGKAFVGEIMNS	±0	nd[h]	−19 400	−24 400	294
MG2+	GIGKFLHSAEKWGKAFVGEIMNS	+2	nd	−15 800	−21 600	281
MG4+	GIGKFLHSAKKWGKAFVGEIMNS	+4	−21 000	−15 100	−19 600	277
MG6+	GIGKFLHSAKKWGKAFVGQIMNSamide	+6	−21 300	−13 000	−11 800	261

[a] The substituted amino acids are underlined. [b] The local pH of the acidic membrane surface is lower (ca. 0.8 pH unit) than that of the bulk (pH 7.0). Therefore, both the α-amino group and the H^7 residue are assumed to be protonated. [c] In deg cm^2 $dmol^{-1}$. Estimation error is ±3%. [d] In egg PG/egg PC (1/1, mol/mol) SUVs at 30 °C. [e] In a TFE/buffer (1/1, v/v) mixture at 11 °C. [f] The van't Hoff enthalpy change upon helix formation, ΔH, in TFE/buffer (1/1). Estimation error is ±500 J/mol. Derived from Figure 4B. [g] The temperature of the midpoint of the transition, T_m, in TFE/buffer (1/1). Estimation error is ±3 K. Derived from Figure 4B. [h] Could not be determined.

Negatively charged acidic phospholipids are necessary for effective binding. (2) The helix essentially lies parallel to the membrane surface (Bechinger et al., 1993; Matsuzaki et al., 1994) because of its equal hydrophobic and hydrophilic angles (Brasseur, 1991). (3) Five helices, together with several surrounding lipids, form a membrane-spanning pore comprising a dynamic, peptide−lipid supramolecular complex, which allows not only the ion transport but also the rapid flip−flop of the membrane lipids (Matsuzaki et al., 1996). The pore-lining lipids make the otherwise insulated outer and inner leaflets a continuum. The pore structure has been recently detected by a neutron diffraction technique (Ludtke et al., 1996). (4) Upon the disintegration of the pore, a fraction of the peptide molecules stochastically translocates into the inner leaflet (Matsuzaki et al., 1995a,b). The pore formation is transient in that it is mainly observable in the very early stage of the peptide−lipid interactions: the reduced peptide density in the outer monolayer resulting from the peptide translocation significantly slows the subsequent pore formation because of its cooperative nature. Furthermore, a quantitative relationship exists between the peptide translocation, the ion efflux, and the lipid flip−flop (Matsuzaki et al., 1996).

In elucidating the basic principles underlying the peptide−lipid interactions, it is important to know how the peptide charge modulates this process. The role of electrostatic interactions between the peptide and the lipid in the peptide binding is well-established (Gawrisch et al., 1993; Kim et al., 1991, Matsuzaki et al., 1991, 1995c; Vaz Gomes et al., 1993). However, no systematic study has been performed about the effects of the peptide charge on the helicity, the pore stability, and the peptide translocation. Specifically, an increase in peptide positive charge will enhance the binding affinity for the negatively charged membrane. On the other hand, it could destabilize the helix and the pore structure composed of several helices because of the electrostatic repulsions between the closely spaced positive charges. For the development of a potent antibiotic (membrane disrupter), an effective membrane binding and a long pore lifetime will be simultaneously achieved. If one utilizes the translocation property of this class of peptide for intracellular drug delivery, a short life span of the pore will be required: the peptide can be effectively internalized without significantly disturbing the membrane barrier.

In this study, we synthesized a series of magainin 2 analogs with different charges (0−6+) whose sequences are summarized in Table 1. A tryptophan (W) residue was introduced at the 12th position to monitor the peptide−lipid interactions. We have confirmed that this substitution does not significantly alter the property of the parent peptide (Matsuzaki et al., 1994). To reduce the positive charge, we substituted glutamic acid (E) residues for lysine (K) residues (MG0 and MG2+). A peptide with an increased positive charge was prepared by the amidation of the two COOH groups of E[19] and the C terminus (MG6+). The binding affinity was monitored on the basis of the tryptophan fluorescence spectra. The helical stability was determined in egg PG/egg PC[1] vesicles or a TFE/buffer mixture by CD spectra. Calcein, a water soluble, anionic fluorescent dye, was employed to estimate the lytic activity of the peptide. Its self-quenching property is also useful in evaluating the lifetime of the pore (Weinstein et al., 1984; Schwarz & Robert, 1992; Matsuzaki et al., 1994; Schwarz & Arbuzova, 1995). The methods to detect the peptide translocation have been recently developed by our laboratory on the basis of RET (Matsuzaki et al., 1995a,b). We found that natural magainin 2 is so designed as to exhibit the maximal lytic activity and that an increase in peptide basicity is a strategy for effective peptide translocation.

MATERIALS AND METHODS

Materials. Magainin 2 analogs were synthesized by a standard Fmoc-based solid phase method. The crude peptides were purified by HPLC and gel filtration (Sephadex G-15, 2.5 × 35 cm column, 0.02 N HCl being used as an eluent), as previously described (Matsuzaki et al., 1991, 1994). The purities of the synthesized peptides were determined by quantitative amino acid analysis and analytical HPLC. The peptide concentration was routinely determined on the basis of the tryptophan UV absorption (Gill & Von Hippel, 1989). Egg PG enzymatically converted from egg PC was a kind gift from Nippon Fine Chemical Co. (Takasago, Japan). Egg PC and fluorescent lipids (DNS-PE and NBD-PE) were purchased from Sigma (St. Louis, MO) and Molecular Probes (Eugene, OR), respectively. Calcein and spectrograde organic solvents were supplied by Dojindo (Kumamoto, Japan). NMR grade TFE was purchased from Aldrich (Milwaukee, WI). All other chemicals from Wako (Tokyo, Japan) were of special grade. A Tris-HCl buffer (10 mM Tris/150 mM NaCl/1 mM EDTA, pH 7.0) was prepared from water twice distilled in a glass still.

[1] Abbreviations: egg PC, egg yolk L-α-phosphatidylcholine; egg PG, L-α-phosphatidyl-DL-glycerol enzymatically converted from egg PC; NBD, 7-nitrobenz-2-oxa-1,3-diazol-4-yl; NBD-PE, *N*-[(7-nitrobenz-2-oxa-1,3-diazol-4-yl)dipalmitoyl]-L-α-phosphatidylethanolamine; DNS-PE, *N*-[[[5-(dimethylamino)naphthyl]sulfonyl]dipalmitoyl]-L-α-phosphatidylethanolamine; Fmoc, fluoren-9-ylmethoxycarbonyl; LUVs, large unilamellar vesicles; SUVs, small unilamellar vesicles; MLVs, multilamellar vesicles; HPLC, high-performance liquid chromatography; NMR, nuclear magnetic resonance; L/P, the lipid to peptide ratio; TFE, 2,2,2-trifluoroethanol; CD, circular dichroism; RET, resonance energy transfer.

Vesicle Preparation. LUVs were prepared by the extrusion of MLVs, as described elsewhere (Matsuzaki et al., 1994). Briefly, a lipid film, after being dried under vacuum overnight, was hydrated with a 70 mM calcein solution for the dye release assay (pH was adjusted to 7.0 with NaOH) or the Tris buffer for the other experiments and vortex-mixed to produce MLVs. The suspension was freeze−thawed for five cycles and then successively extruded through polycarbonate filters (a 0.6 μm pore size filter, 5 times; two stacked 0.1 μm pore size filters, 10 times). SUVs for CD measurements were produced by sonication of the freeze−thawed MLVs in ice/water under a nitrogen atmosphere (Matsuzaki et al., 1989, 1991). The lipid concentration was determined in triplicate by phosphorus analysis (Bartlett, 1959).

Peptide Binding. The binding affinity of the peptide for the membrane was determined on the basis of tryptophan fluorescence. Peptide solutions (2 or 3 μM) containing various amounts of egg PG/egg PC (1/1, mol/mol) LUVs were incubated at 30 °C overnight to reach a binding equilibrium. Fluorescence spectra in the range of 300−400 nm were measured on a Hitachi F-4500 spectrofluorometer at an excitation wavelength of 280 nm. The spectra were corrected for both wavelength-dependent effects (Melhuish, 1962) and intensity loss due to light scattering after subtraction of the corresponding blank spectra without the peptide. The latter correction was carried out by use of indoxyl sulfate (Matsuzaki et al., 1994).

CD Spectra. CD spectra were measured on a Jasco J-720 apparatus interfaced to an NEC PC-9801 microcomputer, using a 1 mm path length quartz cell to minimize the absorbance due to buffer components. The instrumental outputs were calibrated with nonhygroscopic ammonium *d*-camphor-10-sulfonate (Takakuwa et al., 1985). Eight scans were averaged for each sample. The averaged blank spectra (the vesicle suspension or the solvent) were subtracted. For MG4+ and MG6+, the spectra in the membrane-bound form were recorded at 30 °C by use of egg PG/egg PC SUVs. The peptide and the lipid concentrations were 25−30 μM and 0.9−1.0 mM, respectively. The reported spectra were the average of two or three independent preparations. The absence of any optical artifacts was elsewhere confirmed (Matsuzaki et al., 1989). For all peptides, their helical stability was estimated in a TFE/buffer (1/1, v/v) mixture at 10−60 °C. The precise temperature of the cell surface was monitored with a small sensor (Takara Thermister SXK-67, Yokohama, Japan). The peptide concentration was 16−50 μM.

Calcein Leakage. Dye-entrapped LUVs were prepared by hydrating an egg PG/egg PC (1/1) mixture with the 70 mM calcein solution. Calcein-entrapped vesicles were separated from free calcein on a Bio-gel A1.5m column. The release of calcein from the LUVs was fluorometrically monitored on a Shimadzu RF-5000 spectrofluorometer at an excitation wavelength of 490 nm and an emission wavelength of 520 nm at 30 °C. The maximum fluorescence intensity corresponding to 100% leakage was determined by the addition of 10% w/v Triton X-100 (20 μL) to 2 mL of the sample.

RET. Dansyl-labeled LUVs were prepared by hydrating the lipid film composed of egg PG, egg PC, and DNS-PE in a molar ratio of 4:5:1. RET from the tryptophan residue of the peptide to the dansyl chromophore in the membrane was monitored by observing the fluorescence intensity of the tryptophan residue (336 nm) upon excitation at 280 nm. The temperature was controlled at 30 ± 0.5 °C.

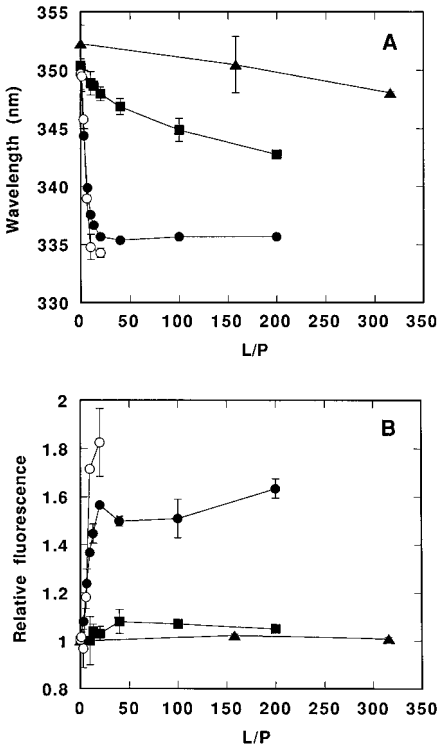

FIGURE 2: Changes in tryptophan fluorescence upon membrane binding. A fixed concentration of a peptide was mixed with various amounts of egg PG/egg PC (1/1) LUVs and incubated at 30 °C overnight for equilibration. The fluorescence spectra were recorded at an excitation wavelength of 280 nm. The maximal wavelength (A) and its intensity (B) are plotted as a function of L/P. Peptide: ○, MG6+; ●, MG4+; ■, MG2+; ▲, MG0.

Dithionite Ion Permeability. A lipid film composed of egg PG/egg PC/NBD-PE (1/1/0.005, mol/mol) was hydrated with the buffer and vortex-mixed. The suspension was freeze−thawed for five cycles. Small aliquots of the MLVs were injected into the buffer (control) or the peptide solution in the presence of 10 mM sodium dithionite. The time course of the NBD fluorescence intensity at 530 nm (excited at 450 nm) was monitored at 30 °C.

RESULTS

Binding Affinity. The effect of the peptide charge on the binding affinity for the membrane was estimated on the basis of the changes in tryptophan fluorescence upon binding. A fixed concentration of the peptide was mixed with various amounts of egg PG/egg PC (1/1) LUVs, and the fluorescence spectra in the equilibrium state were measured. The addition of the vesicles caused a blue shift and a concomitant intensity enhancement, indicating that the fluorophore is buried in a hydrophobic environment of the membrane (Matsuzaki et al., 1994). Isoemissive points were, however, not observed, suggesting that the environments of the fluorophore depend on the peptide density in the membrane phase or the intramembranous aggregational state of the peptide. Although binding isotherms could not be obtained from the spectral changes because of the absence of the simple two-state equilibrium, the dependence of the spectra on L/P gives a measure of the peptide's affinity for the membrane. Figure 2 shows the maximal wavelength (A) and the maximal intensity (B) as a function of L/P. MG6+ (open circles) and MG4+ (closed circles) exhibited the largest binding affinity for the negatively charged membrane. The maximal

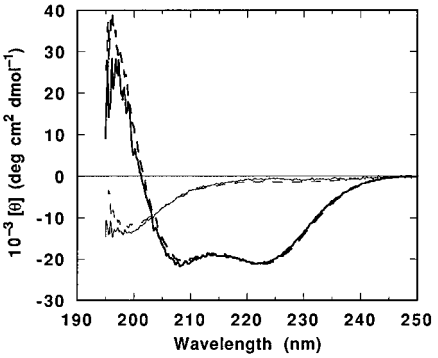

FIGURE 3: CD spectra of MG4+ (solid line) and MG6+ (broken line) at 30 °C. The free form spectra in a 10 mM Tris/150 mM NaCl/1 mM EDTA (pH 7.0) buffer and the membrane-bound form spectra in egg PG/egg PC (1/1) SUVs are shown as thin and thick lines, respectively.

spectral change was observed around L/P = 20. In contrast, the binding of the less basic peptides, MG2+ (closed squares) and MG0 (closed triangles), was much weaker. Thus, the affinity was in the order MG6+ ≥ MG4+ ≫ MG2+ > MG0, suggesting that electrostatic interactions between the positive charge of the peptide and the negative charge of the lipid play a crucial role in the binding process.

Helical Stability. Figure 3 depicts the CD spectra of MG4+ (solid line) and MG6+ (broken line) in the absence or the presence of egg PG/egg PC (1/1) SUVs. In the buffer, both peptides take unordered structures. On the other hand, they conform to helices in the lipidic environment, as characterized by the double minima at 208−209 and 222 nm and a maximum below 200 nm. The spectra are those of the completely membrane-bound form, because further addition of the vesicles did not change the spectra any more. The $[\theta]_{222}$ values were −21 000 and −21 300 deg cm^2 dmol^{-1} (±5%) for MG4+ and MG6+, respectively, indicating that the helicities of both peptides in the membrane are very similar in spite of the different total charges. MG2+ and MG0 also assumed unordered structures in the aqueous medium (data not shown). The spectra of their bound state could not be obtained because of their much weaker binding (Figure 2). Therefore, the helical stability was estimated in a helicogenic, less polar media, i.e., a TFE/buffer (1/1, v/v) mixture. For example, Figure 4A illustrates the CD spectra of MG4+ (50 μM) recorded at 10−60 °C. MG4+ and the other three peptides (spectra not shown) also form helices in this solvent system. The helices appear to be monomeric because the CD spectra measured at a lower concentration (5 μM) were superimposable (data not shown). The helicity was in the order MG0 > MG2+ ≥ MG4+ > MG6+ at lower temperatures (see also Table 1). Isodichroic points around 202 nm were observed for all peptides, demonstrating the presence of just two conformations for each residue, helix and random chain (Padmanabhan et al., 1990). The equilibrium constant, K, can be calculated according to eq 1 (Zhou et al., 1993).

$$K = ([\theta]_h - [\theta])/([\theta] - [\theta]_c) \quad (1)$$

The molar ellipticities at 222 nm of the helix, the helix−coil mixture, and the coil were denoted by $[\theta]_h$, $[\theta]$, and $[\theta]_c$, respectively. The $[\theta]_h$ and $[\theta]_c$ values were assumed to be −37 400 × (1 − 2.5/23) = −33 300 and 0 deg cm^2 dmol^{-1} (Chang et al., 1978).[2] The van't Hoff enthalpy change associated with the coil−helix transition, ΔH, and

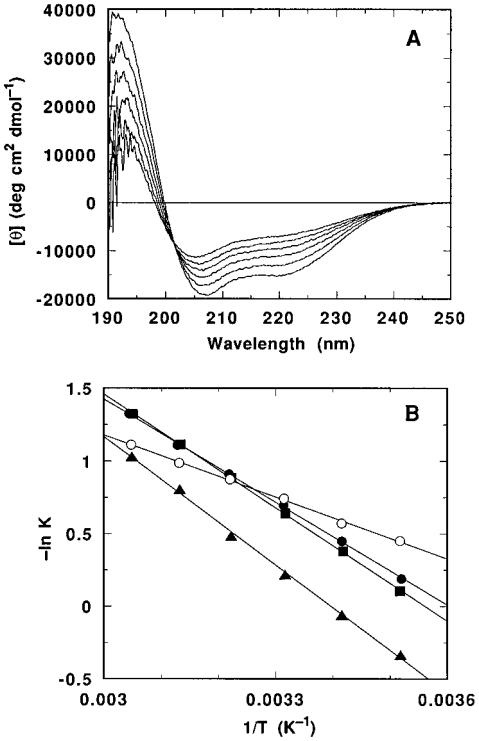

FIGURE 4: Stability of the magainin peptides in a TFE/buffer (1/1, v/v) mixture. (A) CD spectra of MG4+ at 11, 20, 28, 37, 46, and 55 °C, respectively, from the bottom. (B) The van't Hoff plot according to eq 2. Peptide: ○, MG6+; ●, MG4+, ■, MG2+, ▲, MG0. See the text for details.

the temperature at the midpoint of the transition where K = 1, T_m, were evaluated by eq 2.

$$-\ln K = (\Delta H/R)\,(1/T - 1/T_m) \quad (2)$$

The gas constant was denoted by R. Figure 4B shows the −ln K vs 1/T plots. The linearity was good (R > 0.9989). The obtained parameters are summarized in Table 1.

Membrane Permeabilization. The lytic activity of each peptide was assayed on the basis of the efflux of an anionic, fluorescent dye, calcein, from LUVs composed of egg PG/egg PC (1/1). Figure 5 demonstrates the percent leakage value after a 10 min incubation as a function of L/P. The conversion from the observed fluorescence signal to percent leakage requires the knowledge of the lifetime of the pore or the mode of leakage (Schwarz & Arbuzova, 1995), which will be discussed later. The W-substituted analog of wild-type magainin 2, MG4+, exhibited the highest activity: 50% leakage was observed at L/P = 170 (closed circles). The less positive peptide, MG2+, showed a weaker activity (closed squares), less than half that of MG4+, as expected from its weaker binding (Figure 2). The lytic activity of MG0 was extremely weak: an L/P value of around 1 was needed to observe a significant extent of leakage (data not shown). Interestingly, the most basic, highest affinity analog, MG6+, possessed a rather weak potency (open circles), being even less effective than MG2+. The $(L/P)_{50\%}$ value was ca. 50.

[2] One way to experimentally determine $[\theta]_h$ is by TFE titration (Padmanabhan et al., 1990). However, peptides with high positive charges were not soluble in media containing high percentages of TFE. Furthermore, it was recently reported that the helicity of magainin 2 amide does not increase any more at TFE concentrations above 50% (Wieprecht et al., 1996).

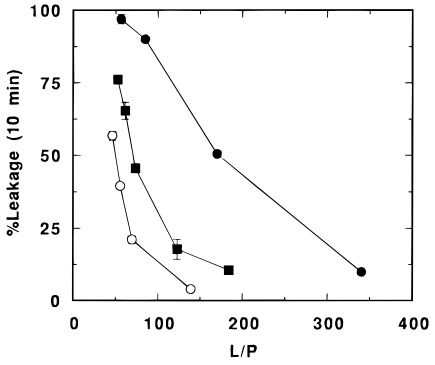

FIGURE 5: The percent leakage of calcein from egg PG/egg PC (1/1) LUVs during 10-min incubation is plotted as a function of L/P ([lipid] = 180 μM). Peptide: ○, MG6+; ●, MG4+; ■, MG2+. The temperature was 30 °C.

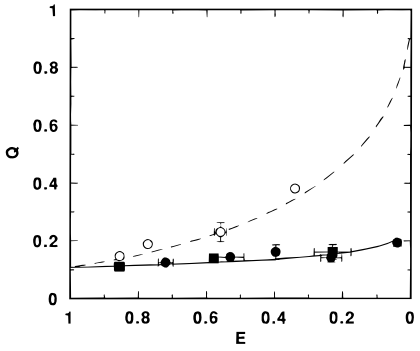

FIGURE 6: Estimation of the pore lifetime at 30 °C. The apparent retention, *E*, is shown against the quenching factor, *Q*. Peptide: ○, MG6+; ●, MG4+; ■, MG2+. The curves are theoretical ones for $\rho = 0.9$ (broken) and 0.1 (solid) calculated according to Schwarz and Arbuzova (1995). See the text for details.

Pore Lifetime. The self-quenching property of calcein was utilized to estimate the life span of the pore. This approach was originally developed by Weinstein et al. (1984) and elaborated by the Schwarz group (Schwarz & Robert, 1992; Schwarz & Arbuzova, 1995). If the lifetime, τ, is much longer than the intrinsic lifetime, τ_0, which is the time necessary for a 1/*e* reduction of the intravesicular dye concentration, a single pore opening is sufficient to exhaust the vesicular contents ("all-or-none mode"). On the other hand, a number of pore openings are necessary to observe a significant extent of leakage in the case of $\tau \ll \tau_0$ ("graded-mode"). There are, of course, many cases between the above two extremes. The τ value can be evaluated by the determination of the extent of self-quenching of the peptide-treated, calcein-entrapped LUVs. After the calcein-containing egg PG/egg PC LUVs were mixed with the peptide at 30 °C, the time course of the calcein fluorescence increase was monitored in a cuvette for 10 min. Aliquots of the liposome suspension were immediately sampled into an Eppendorf tube containing an excess amount of calcein-free LUVs to stop the leakage. Triton X-100 was added to the cuvette to completely lyze the vesicles. The apparent retention, *E*, was calculated according to eq 3.

$$E = (F_t - F)/(F_t - F_0) \quad (3)$$

F and F_t denote the fluorescence intensity before and after the detergent addition, respectively. F_0 represents the fluorescence of the intact vesicle. On the other hand, the liposomes in the Eppedorf tube were applied on a Bio-gel A1.5m column. The vesicle fraction was separated from the leaked calcein by gel filtration, and its quenching factor (Q) was obtained by measuring the fluorescence intensity before (F_b) and after (F_a) the addition of Triton X-100.

$$Q = F_b/F_a \quad (4)$$

The Q value was plotted against the E value in Figure 6.

Schwarz introduced a dimensionless parameter, ρ, to describe the pore life span (Schwarz & Robert, 1992; Schwarz & Arbuzova, 1995).

$$\rho = \tau_0/(\tau + \tau_0) \quad (5)$$

The all-or-none leakage ($\tau \gg \tau_0$) corresponds to $\rho \rightarrow 0$, whereas in the case of the graded mode ($\tau \ll \tau_0$), $\rho \rightarrow 1$. Theoretical Q vs E curves for various ρ values were calculated as reported (Schwarz & Arbuzova, 1995). The comparison of the theory with the data (Figure 6) evaluated the ρ values for MG6+ (open circles), MG4+ (closed circles), and MG2+ (closed squares) to be 0.9, 0.1, and 0.1, respectively, corresponding to $\tau = 0.1\tau_0$, $9\tau_0$, and $9\tau_0$. The estimation error in ρ is ± 0.05.

Peptide Translocation. The translocation of the peptide across the lipid bilayer was detected for MG6+ and MG2+ by the two methods developed by our laboratory. The translocation of MG4+ has already been reported elsewhere (Matsuzaki et al., 1995a,b). The first technique utilizes the extraction of the untranslocated peptide remaining on the outer surface with excess LUVs. The peptide−membrane association was monitored by use of RET from the tryptophan residue to DNS-PE. Figure 7 depicts the results. The experiments were carried out for MG6+ and MG2+ under conditions where approximately 50% leakage was observed for 10 min. In the case of MG6+ (Figure 7A), the addition of DNS-labeled LUVs at time zero reduced the tryptophan fluorescence because of RET. The peptide is completely bound, as judged from Figure 2 (L/P = 47). After 20 s, 1 min, 2 min, or 10 min incubation (traces 2−5), a large excess of the second population of DNS-free vesicles was added, as indicated by the arrows. An abrupt increase in tryptophan fluorescence implies that the peptide which had been bound to the *outer* leaflet of the DNS-LUVs was redistributed between the two populations of the vesicles, being relieved from RET. However, the recovered intensity was always smaller than the intensity (trace 1) when the two kinds of the vesicles were simultaneously added at time zero. The intensity difference is a measure of the translocation. The difference increased with the incubation time, suggesting time-dependent peptide internalization. About 50% of the peptide was translocated during 10 min.[3]

Figure 7B illustrates the results of MG2+. The addition of the DNS-LUVs reduced the fluorescence by only 25% because of the rather weak binding of the peptide (Figure 2). Therefore, the intensity is considered to mainly arise from the free peptide. The enhanced fluorescence intensity after the extraction of the untranslocated peptide was nearly the same as the intensity of the upper trace. The extent of the translocation was at most 10% during a 10 min incubation.

[3] The precise determination of percent translocation for this peptide was difficult, because the extraction was not as rapid as MG4+ because of the stronger electrostatic binding (Figure 7A).

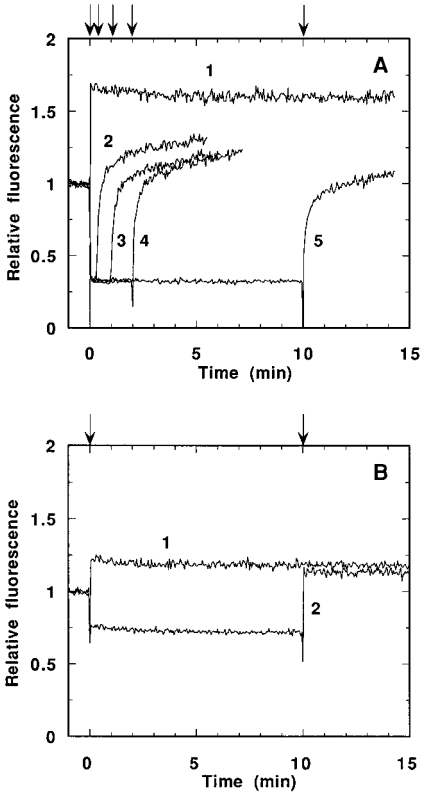

FIGURE 7: Detection of the translocation (1) of MG6+ (A) and MG2+ (B). The peptide was mixed with DNS-LUVs (egg PG/egg PC/DNS-PE = 4/5/1) at time zero. The final peptide concentration was 3 μM, and the lipid concentrations were 140 μM (A) and 185 μM (B). The fluorescence intensity of tryptophan at 336 nm (excited at 280 nm) was recorded. The binding of the peptide to the vesicle reduced the intensity due to RET. At various time intervals of incubation, a large excess (final concentration 1.2 mM) of the second population of DNS-free LUVs (egg PG/egg PC = 1/1) was added, as indicated by the arrows. An increase in intensity indicates the relief from RET caused by the redistribution between the two vesicle populations of the peptide molecules which had been bound to the outer surface of the first vesicle. The increased intensity decreases with prolonged incubation and is smaller than the fluorescence intensity when both populations of vesicles were simultaneously added at time zero (trace 1), thus indicating that a fraction of the peptides translocated into the inner leaflet during the incubation. Each trace is the average of three experiments. Incubation time: (A) trace 2, 0.33 min; trace 3, 1 min; trace 4, 2 min; trace 5, 10 min; (B) trace 2, 10 min. The temperature was controlled at 30 ± 0.5 °C.

Figure 8 shows the other method used to detect the translocation, which uses the NBD-dithionite reaction (McIntyre & Sleight, 1991). Addition of sodium dithionite to the MLVs of egg PG/egg PC (1/1) doped with NBD-PE reduced the chromophores exposed to the external aqueous phase, making them nonfluorescent (trace 1). The extent of quenching was 25−30%, indicating that the lamellarity of the vesicle is ca. 2. The external addition of 2 μM MG6+ (trace 2 in Figure 8A) quenched ~75% fluorescence: the pore formed by MG6+ introduced the $S_2O_4^{2-}$ ions into the first interlamellar space. Further addition of the peptide (7 μM, trace 3) allowed the reducing ion to react with almost all of the NBD groups within 3 min: the peptide molecules translocated across the outermost bilayers to form pores in the *inner bilayers*. In contrast, the maximal fluorescence reduction caused by the addition of MG2+ was 75%, and the kinetics was much slower compared with that of MG6+ (trace 5 in Figure 8B), indicating the less efficient translocation of this peptide, in keeping with Figure 7B.

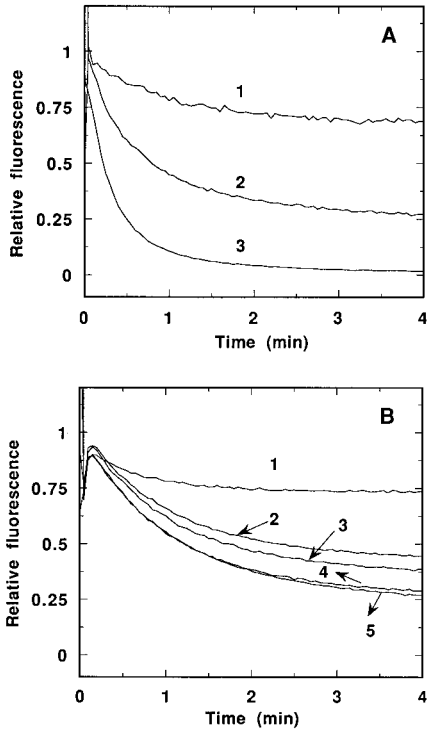

FIGURE 8: Detection of the translocation (2) of MG6+ (A) and MG2+ (B). Small aliquots of MLVs composed of egg PG/egg PC/NBD-PE = 1/1/0.005) were injected into a buffer (curve 1) or a peptide solution (curves 2−5) in the presence of 10 mM sodium dithionite at time zero. The essentially membrane-impermeable ion chemically quenches the NBD fluorescence. The fluorescence at 530 nm (excitation at 450 nm) was normalized to the intensity in the absence of the reducing ion. [lipid] = 100−107 μM. [peptide] (μM): (A) trace 1, 0; trace 2, 2; trace 3, 7; (B) trace 1, 0; trace 2, 3; trace 3, 4; trace 4, 5; trace 5, 7. Note that 7 μM of MG6+ makes almost all NBD groups accessible to the $S_2O_4^{2-}$ ion, suggesting that it passes through the outermost bilayers to form pores in the inner bilayers.

DISCUSSION

Peptide Design and Helical Stability. We synthesized four magainin 2 analogs with different total charges (0−6+) to investigate the effects of peptide charge on the peptide−membrane interactions (Table 1). The local pH of the acidic membrane surface is lower (ca. 0.8 pH unit) than that of the bulk (pH 7.0). Therefore, both the α-amino group and the H^7 residue are assumed to be protonated. The modification was performed by the K to E substitutions or the amidation of the COOH groups of E^{19} and the C terminus. Both derivatizations are expected to never deteriorate the amphiphilic property of magainin 2. Furthermore, the K, E, and Q residues possess similarly high intrinsic helical propensities (Chou & Fasman, 1974; O'Neil & De Grado, 1990; Wôjcik et al., 1990). Thus, these analogs are considered to be useful for the estimation of the effect of peptide charge on the peptide−lipid interactions. All peptides take amphiphilic helices in the membrane or the TFE/water mixture (Figures 3 and 4). The latter solvent system is often used to explore the helical propensities of peptides (Lehrman et al., 1990; Jasanoff & Fersht, 1994; Kemmink & Creighton, 1995). The presence of the isodichroic points suggests a two-state helix−coil transition of each residue (Zhou et al., 1993), whose equilibrium is modulated by side chain interactions. In MG2+, putative E^{10}−K^{14} and H^7−E^{10} ion pairs would stabilize the helix. The additional ion pairs of H^7−E^{11} and E^{11}−K^{14} in MG0 could further

strengthen the helix. The $i-(i+4)$ ion pairs contribute more to the stabilization compared with the $i-(i+3)$ type arrangements (Scholtz et al., 1993). As expected, the stability of the helix in the TFE/buffer system below room temperature is in the order MG0 > MG2+ ≥ MG4+ (Figure 4B, Table 1). However, the stabilization energy is not sufficient for the less positive peptides to form helices in the aqueous environment. Hydrogen bond interactions also exist between the E−K pair other than electrostatic interactions (Scholtz et al., 1993). The latter is considered to more dominantly operate in a media of low dielectric constants. MG6+ with increased repulsions shows a reduced helicity compared with MG4+ (Figure 3) in spite of the fact that the amidation of the C terminus stabilizes the helix because of the elimination of unfavorable Coulomb interactions between the negative charge of COO^- and the helical dipole (Creighton, 1993).

Table 1 shows that the van't Hoff enthalpy change upon the helix formation of this class of peptide is around −0.2 kcal/residue mol, which is comparable with the value (−0.22) of a 50-residue peptide, Ac-Y$(AEAAKA)_8$F-NH_2 in an aqueous buffer containing 0.1 M NaCl (Scholtz et al., 1991). Merutka et al. (1990) reported that the van't Hoff enthalpy changes of 18-residue peptides in a buffer of low ionic strength are ca. −0.5 kcal/residue mol. The ΔH value appears to strongly depend on the peptide sequence and the medium.

The TFE-containing aqueous solution has been also employed as a "membrane-mimetic medium" (e.g., Rizo et al., 1993). However, one should be cautious in that the conformation in the mixed solvent does not necessarily reflect that of the membrane-bound form, as can been seen from Table 1. The helicities of MG4+ and MG6+ bound to the membranes are much higher than those in the mixed solvent. Furthermore, the differences in helical propensity between the two peptides predicted in the latter medium is not reflected in the former system.

The group of Dathe (1996) recently compared the conformations of double-D-substituted magainin 2 amide analogs in various media. In a TFE/buffer system, the magainin 2 amide helix is most stable in the region of $F^{16}-E^{19}$, suggesting that the involvement of the unique negative charge of E^{19} in the helix stabilization. Similarly, the modification of MG4+ → MG6+ causes the largest changes in the thermodynamic parameters (Table 1). Therefore, not only the net charge but also the position of the substitution affects the helix stability. In contrast to the solvent system, the helix of magainin 2 amide is uniformly stable in the sequence of 9−19 in lipid bilayers. Furthermore, the conformation of the membrane-bound state is almost independent of the membrane surface charge, indicating that, in the lipid matrix, hydrophobic interactions between the apolar face of the amphiphilic helix and the hydrocarbon chains of the lipid, rather than the side chain electrostatic interactions, regulate the helical stability. Thus, the helices of our magainin analogs appear to be equally stable in the membrane, as observed for MG4+ and MG6+ (Figure 3).

Binding and Pore Formation. The affinity of the peptide for the negatively charged membrane augments with the positive charge of the peptide (Figure 2), strengthening the importance of electrostatic interactions in the binding process (Gawrisch et al., 1993; Kim et al., 1991; Matsuzaki et al., 1991, 1995c; Vaz Gomes et al., 1993). This fact can explain, at least in part, the stronger lytic activity of MG4+ than that of MG2+ and MG0. In spite of the tighter binding, MG6+ exhibited the leakage even weaker than MG2+, suggesting the presence of pore-destabilizing factors.

The life span of the MG6+ pore ($0.1\tau_0$) is significantly shorter than those of MG4+ and MG2+ ($9\tau_0$, Figure 6).[4] It should be noted here that the τ_0 value itself may depend on the peptide charge: the anionic dye could more rapidly pass through the highly positive pore. The τ_0 value is estimated to be on the order of 10 ms, if one ignores the electrostatic interactions between the dye and the pore wall (Matsuzaki et al., 1995b). Furthermore, τ_0 is inversely proportional to the pore radius, which might differ from peptide to peptide. However, the pore sizes are considered to be similar among the peptides investigated, because we employed calcein of definite size as a marker. In our previous paper (Matsuzaki et al., 1994), the calcein leakage induced by MG4+ from egg PG LUVs was reported to occur in the graded mode ($\rho \approx 1$). The lipid composition may also influence both τ_0 and τ, because the lipid molecules are involved in the pore structure (Matsuzaki et al., 1996). In conclusion, the lifetime of the pore is also modulated by the charge density of the pore wall and appears to be in the order MG2+ ≥ MG4+ ≫ MG6+. The weak lytic power of MG6+ can be ascribed to the fact that its monomer pore equilibrium lies so far on the monomer side. The unstability of the pore formed by the highly basic peptide is mainly due to interhelical electrostatic repulsions rather than the stability of the helix per se (vide supra). The length of a 23-residue helix is ca. 3.5 nm. Four lipid molecules can dimensionally flank one side of the helix, assuming a surface area per lipid of 0.68 nm^2. If the pore is composed of alternating arrays of the peptide and the lipid, the maximum positive charge that the anionic lipids can neutralize is 4. Therefore, the MG6+ pore can be considerably unstable.

Translocation. According to our scheme (Matsuzaki et al., 1995a,b), the peptide with a shorter lifetime can more effectively translocate across the bilayer, because the peptide

[4] It is plausible that MG6+ translocates via membrane perturbation. However, we consider that the MG6+ pore structure is essentially similar to that of the MG4+ pore based on the following reasons, although the MG6+ pore may be less well-defined than the MG4+ pore, as judged from the shortest lifetime. (1) The peptide molecules are completely membrane-bound and form helices under our experimental conditions. Therefore, the membrane permeation of the free peptide through a defect caused by the peptide-induced membrane perturbation is unrealistic. (2) The pore should be an intermediate structure during the translocation. The pore model (Figure 1B) avoids the unfavorable exposure of the polar side chains to the hydrophobic interior of the bilayer.

[5] We discussed, on the basis of Schwarz's quantitative treatment, that the incorporation of egg PC into egg PG membranes shortens the pore lifetime (Matsuzaki et al., 1995b). However, this estimation does not agree with the observed life span (Figure 6).

[6] To explain the observed coupling between the calcein efflux and the lipid flip−flop, we employed the model (Matsuzaki et al., 1996) in which the lipid molecules two-dimensionally diffuse through the perimeter of the pore, $2\pi r$ (r: pore radius), using the approximation that the number of the lipid molecules per pore is much larger than 2 (see eq A8). The actual situation would be that the lipid number is equal to or smaller than the number of the helices (5). In this case, the effective diffusion path is significantly shorter than $2\pi r$. Therefore, the sum of the shorter routes of both the dye-permeable and -impermeable pores may happen to be ca. $2\pi r$ in average.

[7] This conclusion apparently does not hold as for the magainin−Gram-negative bacteria interactions. MG6+ possesses a stronger antimicrobial activity than MG4+. This observation can be explained by the fact that the interactions of the peptides with outer membranes of Gram-negative bacteria are more important than those with cytoplasmic membranes whose fundamental architecture is phospholipid bilayers (Matsuzaki, et al., unpublished work).

is internalized only upon the disintegration of the pore. Therefore, the translocation ability is expected to be in the order of MG6+ ≫ MG4+ ≥ MG2+. Let us compare the degree of the translocation at L/P ratios of 50−60. MG6+ crosses the bilayer most efficiently (Figures 7 and 8). The peptide reached a 50−50% equilibrium distribution between the two leaflets during 10 min under the conditions where 55% leakage was observed. In contrast, the extent of translocation for MG4+ was only 20−30% under 80% leakage conditions (Matsuzaki et al., 1995a). The membrane permeation of MG2+ could hardly be detected (Figures 7 and 8). The weaker binding of MG2+ seems to deteriorate its intrinsic inefficient translocation.

Although the above argument on the relationship between the pore stability and the translocation efficiency is qualitatively satisfactory, the quantitative treatment remains to be improved.[5] According to Schwarz's theory (Schwarz & Robert, 1992), the number of pores per vesicle which had been formed from $t = 0$ to t, $p(t)$, can be expressed by eq 6.

$$p(t) = -\{\ln(1 - L(t))\}/(1 - \rho) \quad (6)$$

The extent of leakage was denoted by $L(t)$ ($0 \leq L(t) \leq 1$). For example, in the case of MG6+ ($\rho = 0.9$), $p(10\ \text{min}) = 8$ at $L(t) = 0.55$. Assuming a pentameric pore, this means that only 40 peptide molecules had formed the pore during the incubation, whereas the number of MG6+ molecules which had translocated is approximately 1000 (Figure 7A). The large discrepancy may be attributed to the following possibilities: (1) The peptide translocates also through the aqueous pore in its unfolded state. This case is less plausible at least in the MG6+ and MG4+ systems where most peptides are membrane-bound. (2) A major fraction of the peptide crosses the membrane by forming a calcein-impermeable, smaller pore. Our previous studies revealed that a magainin pore is composed of five helices and several lipid molecules (Matsuzaki et al., 1995 a,b, 1996). It is plausible that the number of the intercalated lipids per pore has a distribution. A larger pore comprising five helices and several lipid molecules can permeate the dye, whereas a smaller pore containing fewer lipids cannot. On the other hand, the peptide translocation (and the lipid flip−flop) equally occurs via both pores.[6]

CONCLUSIONS

Using a series of magainin 2 analogs with different charges, we clarified that an increase in the positive charge enhances the binding of the peptide to the acidic phospholipid membrane, whereas it shortens the pore lifetime, thus promoting the translocation. The charge distribution of wild-type magainin 2 is so designed as to maximize the lytic activity with the relatively strong binding and the moderate pore lifetime.[7] A designed peptide with a large positive charge would exhibit a high translocation ability without significantly damaging the barrier property of the membrane.

REFERENCES

Bartlett, G. R. (1959) *J. Biol. Chem. 234*, 466−468.

Bechinger, B., Zasloff, M., & Opella, S. J. (1993) *Protein Sci. 2*, 2077−2084.

Brasseur, R. (1991) *J. Biol. Chem. 266*, 16120−16127.

Chang, C. T., Wu, C.-S. C., & Yang, J. T. (1978) *Anal. Biochem. 91*, 13−31.

Chou, P. Y., & Fasman, G. D. (1974) *Biochemistry 13*, 211−222.

Creighton, T. E. (1993) in *Proteins. Structures and Molecular Properties* pp 182−186, W. H. Freeman and Co., New York.

Gawrisch, K., Han, K.-H., Yang, J.-S., Bergelson, L. D., & Ferreti, J. A. (1993) *Biochemistry 32*, 3112−3118.

Gill, S. C., & Von Hippel, P. H. (1989) *Anal. Biochem. 182*, 319−326.

Grant, E., Jr., Beeler, T. J., Taylor, K. M. P., Gable, K., & Roseman, M. A. (1992) *Biochemistry 31*, 9912−9918.

Jasanoff, A., & Fersht, A. R. (1994) *Biochemistry 33*, 2129−2135.

Kemmink, J., & Creighton, T. E. (1995) *Biochemistry 34*, 12630−12635.

Kim, J., Mosior, M., Chung, L. A., Wu, H., & McLaughlin, S. (1991) *Biophys. J. 60*, 135−148.

Lehrman, S. R., Tuls, J. L., & Lund, M. (1990) *Biochemistry 29*, 5590−5596.

Ludtke, S. J., He, K., Heller, W. T., Harroun, T. A., Yang, L., & Huang, H. W. (1996) *Biochemistry 35*, 13723−13728.

Maloy, W. L., & Kari, U. P. (1995) *Biopolymers 37*, 105−122.

Matsuzaki, K., Nakai, S., Handa, T., Takaishi, Y., Fujita, T., & Miyajima, K. (1989) *Biochemistry 28*, 9392−9398.

Matsuzaki, K., Harada, M., Funakoshi, S., Fujii, N., & Miyajima, K. (1991) *Biochim. Biophys. Acta 1063*, 162−170.

Matsuzaki, K., Murase, O., Tokuda, H., Funakoshi, S., Fujii, N., & Miyajima, K. (1994) *Biochemistry 33*, 3342−3349.

Matsuzaki, K., Murase, O., Fujii, N., & Miyajima, K. (1995a) *Biochemistry 34*, 6521−6526.

Matsuzaki, K., Murase, O., & Miyajima, K. (1995b) *Biochemistry 34*, 12553−12559.

Matsuzaki, K., Sugishita, K., Fujii, N., & Miyajima, K. (1995c) *Biochemistry 34*, 3423−3429.

Matsuzaki, K., Murase, O., Fujii, N., & Miyajima, K. (1996) *Biochemistry 35*, 11361−11368.

McIntyre, J. C., & Sleight, R. G. (1991) *Biochemistry 30*, 11819−11827.

Melhuish, W. H. (1962) *J. Opt. Soc. Am. 52*, 1256−1258.

Merutka, G., Lipton, W., Shalongo, W., Park, S.-H., & Stellwagen, E. (1990) *Biochemistry 29*, 7511−7515.

O'Neil, K. T., & De Grado, W. F. (1990) *Science 250*, 646−651.

Padmanabhan, S., Marqusee, S., Ridgeway, T., Laue, T. M., & Baldwin, R. L. (1990) *Nature 344*, 268−270.

Rizo, J., Blanco, F. J., Kobe, B., Bruch, M. D., & Gierasch, L. M. (1993) *Biochemistry 32*, 4881−4894.

Scholtz, J. M., Marqusee, S., Baldwin, R. L., York, E. J., Stewart, J. M., Santoro, M., & Bolen, D. W. (1991) *Proc. Natl. Acad. Sci. U.S.A. 88*, 2854−2858.

Scholtz, J. M., Qian, H., Robbins, V. H., & Baldwin, R. L. (1993) *Biochemistry 32*, 9668−9676.

Schwarz, G., & Robert, C. H. (1992) *Biophys. Chem. 42*, 291−296.

Schwarz, G., & Arbuzova, A. (1995) *Biochim. Biophys. Acta 1239*, 51−57.

Takakuwa, T., Konno, T., & Meguro, H. (1985) *Anal. Sci. 1*, 215−218.

Vaz Gomes, A., de Waal, A., Berden, J. A., & Westerhoff, H. V. (1993) *Biochemistry 32*, 5365−5372.

Wade, D., Boman, A., Wåhlin, B., Drain, C. M., Andreu, D., Boman, H. G., & Merrifield, R. B. (1990) *Proc. Natl. Acad. Sci. U.S.A. 87*, 4761−4765.

Weinstein, J. N., Ralston, E., Leserman, L. D., Klausner, R. D., Dragsten, P., Henkart, P., & Blumenthal, R. (1984) in *Liposome Technology* (Gregoriadis, G., Ed.) pp 183−204, CRC Press, Boca Raton, FL.

Wieprecht, T., Dathe, M., Schümann, M., Krause, E., Beyermann, M., & Bienert, M. (1996) *Biochemistry 35*, 10844−10853.

Wôjcik, J., Altmann, K.-H., & Scheraga, H. A. (1990) *Biopolymers 30*, 121−134.

Zasloff, M. (1987) *Proc. Natl. Acad. Sci. U.S.A. 84*, 5449−5453.

Zhou, N. E., Kay, M. K., Sykes, B. D., & Hodges, R. S. (1993) *Biochemistry 32*, 6190−6197.

BI961870P